ELSEVIER

Contents lists available at ScienceDirect

### Computers and Chemical Engineering

journal homepage: www.elsevier.com/locate/compchemeng



# Optimization of a reactive distillation process with intermediate condensers for silane production



J. Rafael Alcántara-Avila<sup>a</sup>, Hugo Alberto Sillas-Delgado<sup>b</sup>, Juan Gabriel Segovia-Hernández<sup>b,\*</sup>, Fernando I. Gómez-Castro<sup>b</sup>, Jorge A. Cervantes-Jauregui<sup>c</sup>

- <sup>a</sup> Department of Chemical Science and Technology, Tokushima University, 2-1 Minami Josanjima-cho, Tokushima 770-8506, Japan
- <sup>b</sup> Departamento de Ingeniería Química, División de Ciencias Naturales y Exactas Universidad de Guanajuato, Campus Guanajuato, Noria Alta s/n, Guanajuato 36050, Mexico
- <sup>c</sup> Departamento de Química, División de Ciencias Naturales y Exactas Universidad de Guanajuato, Campus Guanajuato, Noria Alta s/n, Guanajuato 36050, Mexico

#### ARTICLE INFO

Article history: Received 29 August 2014 Received in revised form 18 February 2015 Accepted 15 April 2015 Available online 23 April 2015

Keywords: Reactive distillation Silanes Intermediate condensers Optimization

#### ABSTRACT

This work presents a reactive distillation column for the catalytic disproportionation of trichlorosilane to silane which includes three consecutive reversible reactions. This reaction system is however characterized by a large distinction in the boiling points of the components, which make the reactive distillation extremely favored. Nevertheless, the normal reactive distillation column possesses the shortage of high refrigeration requirement. By removing heat at temperature higher than that at the condenser a superstructure representation, rigorous simulations, and optimization problems were combined to derive optimal reactive distillation columns which can realize heat integration between stages and utilities at several refrigeration conditions. An iterative simulation-optimization procedure was proposed to consider temperature changes in stages due to heat integration. The results showed that the installation of two inter-condensers results in the best option with economic savings up to 56%.

© 2015 Elsevier Ltd. All rights reserved.

#### 1. Introduction

Global power consumption currently stands at approximately 15 TW, the vast majority of which is generated by the combustion of fossil fuels. The associated release of CO<sub>2</sub> from these anthropogenic sources has dramatically altered the composition of the atmosphere and may detrimentally impact global temperature, sea levels, and weather patterns (Parida et al., 2011). Furthermore, the realization that fossil fuels are not inexhaustible and that enhancing recovery of coal, oil and natural gas presents additional risks, drive energy policy scenarios that are based on renewable forms of energy. In most of the proposed scenarios, solar energy is the primary constituent as it is the major energy source over large regions. Solar energy in addition to maintaining life on the planet, is used on demand in three basic forms based on anthropogenic processes: Electricity from the direct conversion of solar energy using semiconductor materials (solar photovoltaics,

PV); electricity from captured thermal energy (concentrated solar power), and heat from the sun (solar thermal). Overall, the market for photovoltaics has been growing at an average rate of 45% per year over the past decade (Braga et al., 2008; Huang et al., 2013).

The five year growth rate from 2007 to 2011 was approximately 70% per year, but this was slowed down to 15% in 2012 as the incentives in several European countries were reduced. While the growth numbers are very impressive, the 27 GW installed in 2011 is just a fraction of one percent of the total amount of electricity that was generated by all sources, indicating that there is plenty of room for further growth (Müller et al., 2006). Photovoltaics use semiconductor materials to generate electricity from solar energy. A semiconductor is a solid, mostly crystalline, material such as silicon, selenium or germanium. Semiconductors have electrical conductivities greater than insulators but lower than metals which are good conductors. At low temperatures and high level of purity, they are insulators but at high temperatures and/or when they are doped and excited by sunlight, they conduct electrons. The most commonly used semiconductor element is silicon. Therefore silicon, the starting material for the crystalline wafer, today is the most important material in PV industry (Fthenakis et al., 2009).

<sup>\*</sup> Corresponding author. Tel.: +52 473 732 0006x8142. E-mail address: gsegovia@ugto.mx (J.G. Segovia-Hernández).

To widely commercialize the solar technology, one challenge faced by the PV industry is to decrease the manufacturing costs, especially the cost of solar-grade silicon feedstock material. The most well-known chemical route to produce solar-grade silicon is the Siemens process, which performs decomposition at about 1000 °C of trichlorosilane by Chemical Vapor Deposition. However, the extremely high consumption of electrical energy as well as the corrosion caused by the byproduct (hydrochloric acid) in some way has limitations in the production of low-cost polysilicon.

The silane pyrolysis process operated in a continuous fluidized bed reactor for its low consumption of energy is an alternative (Iya, 1989; Flagella, 1992). In order to reduce the temperature of silicon deposition, silane (SiH<sub>4</sub>) is used as starting source in the CVD reactor. Other very well known route to produce silane is the disproportionation reactions of SiHCl<sub>3</sub> involving the formation of dichlorosilane (SiH<sub>2</sub>Cl<sub>2</sub>) and monochlorosilane (SiH<sub>3</sub>Cl) as intermediates and tetrachlorosilane (SiCl<sub>4</sub>) as by product (Bakay, 1976). The conventional process for highly pure silane production from trichlorosilane disproportionation is through two reactors and several separation units. However, due to unfavorable chemical equilibrium, this reaction and separation process requires an extremely large recycle ratio and thus the cost of energy as well as investment is very high (Breneman, 1987).

In this context, Reactive Distillation (RD) is particularly attractive for reactions limited by chemical equilibrium, and it can be suitable for the disproportionation reactions because it eliminates conversion and phase equilibrium limitations by continuous removal of products from the reaction zone unit (Sundmacher and Kienle, 2003).

Reactive distillation is a combination of separation and reaction in a single vessel. The concept of combining these two important functions for enhancement of overall performance is an important concept in chemical engineering. The commercial success of reactive distillation for the production of MTBE was immediately followed by another remarkable achievement with the Eastman Kodak process that condensed the whole chemical plant for methyl acetate in a single reactive distillation unit (Sundmacher and Kienle, 2003).

In some applications, particularly in cases where thermodynamic reaction equilibrium prevents high conversions, the coupling of distillation to remove the reaction products from the reaction zone can significantly improve the overall conversion and selectivity at pressures and temperatures that are compatible with the distillation conditions. In other applications, the presence of reactions is used to overcome the separation problems caused by the presence of azeotropes. Therefore, this combination of reaction and distillation often results into simpler and intensified processes with less recycle streams, reduced waste handling and, as a consequence, lower investment and operating costs (Carrera-Rodríguez et al., 2011)

Some important references related to reactive distillation and silanes production can be described. Bakay (1976) proposed in a patent, the process for manufacturing silane in a bed of anion exchange resin by controlling the top temperature between the boiling points of silane and trichlorosilane. In such process, silane could be produced directly from trichlorosilane in a single step process wherein a solid redistribution catalyst also served as the contact surface in a fractional distillation column. The Bakay's patent, although it was not so named as Reactive Distillation, the process was "the essential embodiment because that both chemical reaction and distillation separation were conducted in the same apparatus" (Breneman, 2013).

Yamada et al. (1984) described a process using amines as homogeneous catalysts. Inoue (1988) reported in a patent a Reactive distillation process for dichlorosilane redistribution to silane, trichlorosilane and tetrachlorosilane. Matthes et al. (1988)

**Table 1**Binary interaction parameters (Huang et al., 2013).

i	j	$k_{ij}$	
SiCl <sub>4</sub>	SiHCl <sub>3</sub>	0.01603	
SiCl <sub>4</sub>	SiH <sub>2</sub> Cl <sub>2</sub>	0.02108	
SiHCl <sub>3</sub>	SiH <sub>2</sub> Cl <sub>2</sub>	0.05183	
SiH <sub>2</sub> Cl <sub>2</sub>	SiH₃Cl	-0.00538	
SiH₃Cl	SiH <sub>4</sub>	0.000953	

and Frings (2000) reported a distillation process with a coupled reactor for trichlorosilane redistribution to dichlorosilane and tetrachlorosilane.

Later, Müller et al. (2002) studied potential reactive distillation schemes for silane production without paying attention to the generation of intermediate reaction products.

Muller et al. (2005) and Block et al. (2005) with Solarworld AG suggested some reactive distillation schemes with intercondensers. Sonnenschein et al. (2011) with Envonik Degussa presented a distillation column with a side reactor.

It can be considered that one of the major disadvantages in using reactive distillation for the disproportionation of trichlorosilane is the low boiling point of the target product at the top of the column (silane), which is around  $-112\,^{\circ}\text{C}$  and enforces the use of refrigeration services to condensate it. To alleviate this issue, recently, the use of intermediate condensers has been proposed to reduce the energy consumption and cost of the refrigeration service at the top of the column (Muller et al., 2005; Huang et al., 2013).

On the other hand, Huang et al. (2013) have reported a design procedure to derive feasible reactive distillation columns for silane production from trichlorosilane by means of sensitivity analysis, a trial-and-error method, and some arbitrary assumptions. In addition, Breneman (2013) proposed the used of reactive distillation for the production of several hydrohalosilanes, however, the design analysis in terms of energy consumption was not considered, therefore there is a good area for energy and cost reduction in the aforementioned reactive distillation schemes.

In this work, we investigate the feasibility of applying reactive distillation to the production of silane through the disproportionation of trichlorosilane. This reaction system is however characterized by a large distinction in the boiling points of the components, which makes the reactive distillation extremely favored. Nevertheless, the normal reactive distillation column possesses the shortage of high refrigeration requirement due to the standard boiling point of the overhead product. The design and optimization of reactive distillation column with inter-condensers has been studied as a feasible alternative to alleviate this drawback.

#### 2. Case study

The production of silane ( $SiH_4$ ) through disproportionation of thrichlorosilane ( $SiHCl_3$ ) in a reactive distillation column has been studied. The reaction occurs in three steps, having as intermediates dichlorosilane ( $SiH_2Cl_2$ ) and monochlorosilane ( $SiH_3Cl$ ) and as byproduct chlorosilane ( $SiCl_4$ ), as follows:

$$2SiHCl_3 \leftrightarrow SiH_2Cl_2 + SiCl_4 \tag{1}$$

$$2SiH_2Cl_2 \leftrightarrow SiH_3Cl + SiHCl_3 \tag{2}$$

$$2SiH_3Cl \leftrightarrow SiH_4 + SiH_2Cl_2 \tag{3}$$

The vapor-liquid equilibrium has been modeled using the Peng–Robinson equation of state, with the binary interaction parameters shown in Table 1.

The reaction occurs in liquid phase, using as catalyst the polymeric resin Amberlyst A-21. For the disproportionation of

**Table 2** Parameters required for the calculation of reaction rates (Huang et al., 2013).

I	$k_{0,I}$ (s <sup>-1</sup> )	E <sub>A</sub> (J/mol)	$K_{\rm EQ0,I}$	ΔH (J/mol)
1	73.5	30,045	0.1856	6402
2	949,466.4	51,083	0.7669	2226
3	1176.9	26,320	0.6890	-2548

trichlorosilane using such catalyst, the next pseudo-homogeneous kinetic model has been proposed (Li, 1988; Huang et al., 2013):

$$r_1 = k_1 \left( x_{\text{TCS}}^2 - \frac{x_{\text{STC}} x_{\text{DCS}}}{K_{\text{EQ},1}} \right) \tag{4}$$

$$r_2 = k_2 \left( x_{\text{DCS}}^2 - \frac{x_{\text{TCS}} x_{\text{MCS}}}{K_{\text{EQ},2}} \right)$$
 (5)

$$r_3 = k_3 \left( x_{\text{MCS}}^2 - \frac{x_{\text{DCS}} x_{\text{SIL}}}{K_{\text{EQ},3}} \right)$$
 (6)

where subscripts STC, TCS, DCS, MCS, SIL stands for silicon tetrachloride, trichlorosilane, dichlorosilane, monochlorosilane and silane, respectively. Numerical subscripts correspond to the reactions shown in Eqs. (1)–(3), respectively. Variation of the kinetic constant ( $k_{\rm I}$ ) and equilibrium constant ( $K_{\rm EQ,I}$ ) with temperature are given by Arrhenius' equations (Huang et al., 2013):

$$k_{\rm I} = k_{0,\rm I} e^{-E_A/RT} \tag{7}$$

$$K_{\text{EQ,I}} = K_{\text{EQ0,I}} e^{-\Delta H/RT} \tag{8}$$

where  $k_{0,\mathrm{I}}$  and  $K_{\mathrm{EQ0,I}}$  are the pre-exponential factors for the kinetic constant and the equilibrium constant, respectively;  $E_A$  is the activation energy for the forward reaction,  $\Delta H$  is the heat of reaction and T is the absolute temperature. Constants required for the calculation of reaction rates are shown in Table 2. It can be noticed that the reaction where dichlorosilane is decomposed into monochlorosilane is considerably faster than the other two reactions.

To model the reactive distillation column, the RadFrac module of the commercial process simulator Aspen Plus V8.0 has been used. The feed stream has a flow rate of 10 kmol/h of pure trichlorosilane, and enters to the column at 557 kPa and 50 °C. Silane is obtained at the top of the column with a purity of 99 mol%, while silicon tetrachloride is the bottoms product, with a purity of 99 mol%. The condenser operates at 506 kPa, with a pressure drop of 0.5 kPa per stage. A representation of a reactive distillation column is shown in Fig. 1a. Since the condenser operated at temperatures lower than

**Table 3**Utilities used for cooling and heating.

Utility ID	Inlet temperature (°C)	Outlet temperature (°C)	Utility cost (\$/MWh)
R1	-88	-88	151.94
R2	-30	-30	34.67
R3	-20	-20	28.40
CHW	5	15	15.95
CW	30	40	1.274
MS	160	160	50.58

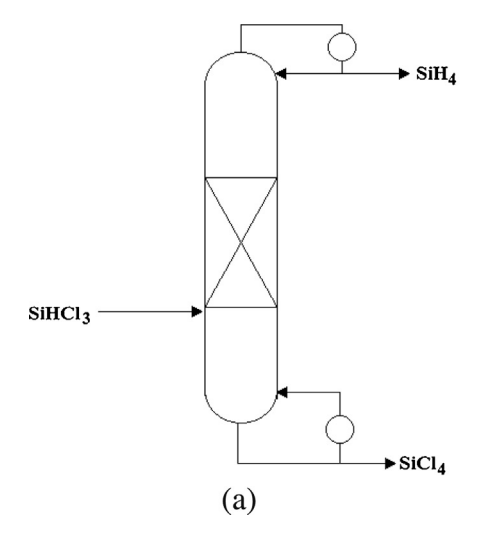
 $0\,^{\circ}$ C, the use of refrigerant is necessary, increasing the cost of the separation. To reduce the cooling duty at the condenser, the use of intermediate heat exchangers is investigated in the next section. A representation of a reactive distillation column with a single intermediate exchanger is shown in Fig. 1b.

#### 3. Installation of inter-condensers in reactive distillation

In distillation columns, whether there is a reaction section or not, the vapor stream leaving at the top of the column must be condensed at the lowest temperature condition while the liquid stream leaving at the bottom of the column must be heated at the highest temperature condition. In this work, since silane is obtained at the top, it must be condensed at about  $-78\,^{\circ}\text{C}$  which results in the use of an expensive refrigeration system to provide cooling at temperatures below  $-85\,^{\circ}\text{C}$ . Typically, to avoid condensing at such low temperature levels, the column operating pressure could be increased, however, this option would be impractical because catalyst deactivation at high pressure.

This section exploits the idea of cooling at higher temperatures than that at the condenser allowing the use of less expensive cooling utilities. The cooling and heating utilities used in this research are shown in Table 3 where R1, R2, and R3 denote refrigeration systems at three different temperatures, CHW and CW denote chilled and cooling water, respectively, and MS denotes steam at middle pressure (618 kPa).

Fig. 2 shows the temperature profile in a column which has 64 stages where the feed is located at stage 26 and the reaction section is between stages 16 and 45. The condenser duty ( $Q^{cn}$ ) and the reboiler duty ( $Q^{rb}$ ) are shown in Fig. 2. In addition, it can be seen how stages 1 (the condenser) and 2 can only be cooled by R1, stages 3 through 15 can be cooled by R2 or R3, stages 16 and 17 can be cooled by CHW, and stages 18 through 25 can be cooled by CW. At first glance, the selection of the best locations and utilities for heat



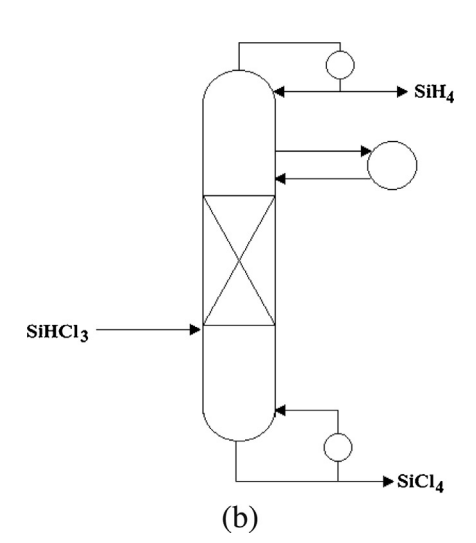


Fig. 1. (a) Reactive distillation column. (b) Reactive distillation column with an intermediate heat exchanger.

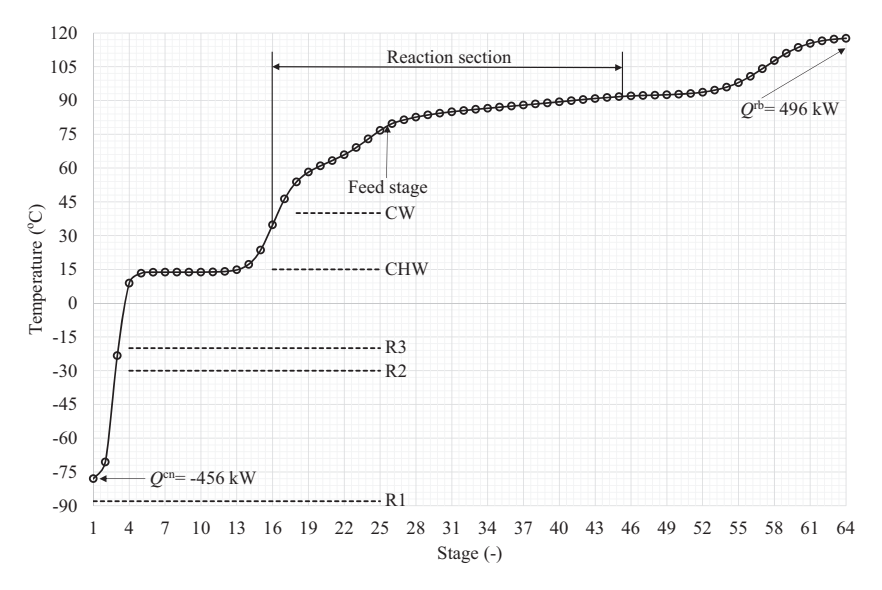


Fig. 2. Candidate cooling utilities for a reactive distillation column without heat-integrated stages.

integration does not look complicated, however, there are two very important features to consider in heat-integrated stages:

- The heat removed or added at a stage in a rectifying or stripping section is not equal to the net condenser or reboiler duty reduction.
- The heat removed or added at stages alters their vapor-liquid equilibrium composition, thus the temperature profile changes in the column.

To clarify the abovementioned points, Fig. 3 shows the case where 100 kW are removed at stage 16 and 300 kW at stage 18. It can be seen that despite CHW seems a candidate cooling utility at stage 16, actually it cannot be used to remove 100 kW because the temperature difference between stage 3 and CHW is less than  $\Delta T_{\rm min}$ . Similarly, CW cannot be used to remove 300 kW because its temperature difference between stage 18 and CW is less than  $\Delta T_{\rm min}$ . In addition, it is demonstrated that despite 400 kW are removed in the stripping section, only 384 kW are successfully removed at the condenser. It can be said that 16 kW are inefficiently removed at the condenser and that results in an increase at the

reboiler duty. The next subsection shows the optimization procedure to minimize the operating cost in a reactive distillation column where the installation of inter-condensers and inter-reboilers is possible.

## 3.1. Mathematical formulation for the installation of inter-condensers and inter-reboilers in reactive distillation

Fig. 4 shows a superstructure representation for a given reactive distillation column where cooling and heating are possible at locations other than the condenser in the rectifying section and the reboiler in the stripping section, respectively. This superstructure comprises all the possible cooling and heating candidate utilities shown in Table 3. The installation of inter-condensers and interreboilers affect both the reaction rate and vapor—liquid equilibrium which results in changes of the equipment size and in operating conditions. The superstructure in Fig. 4 can be formulated as an optimization problem which minimizes the energy consumption in a reactive distillation column with inter-condensers and interreboilers.

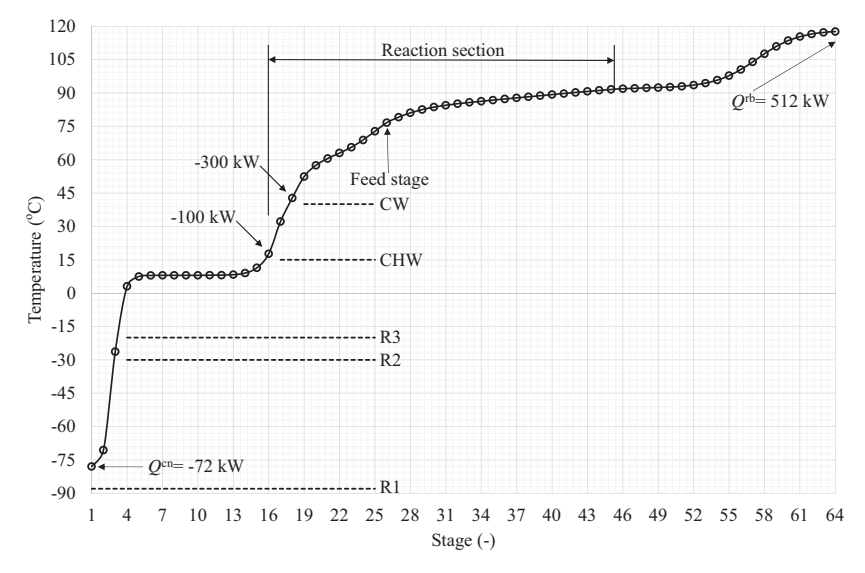
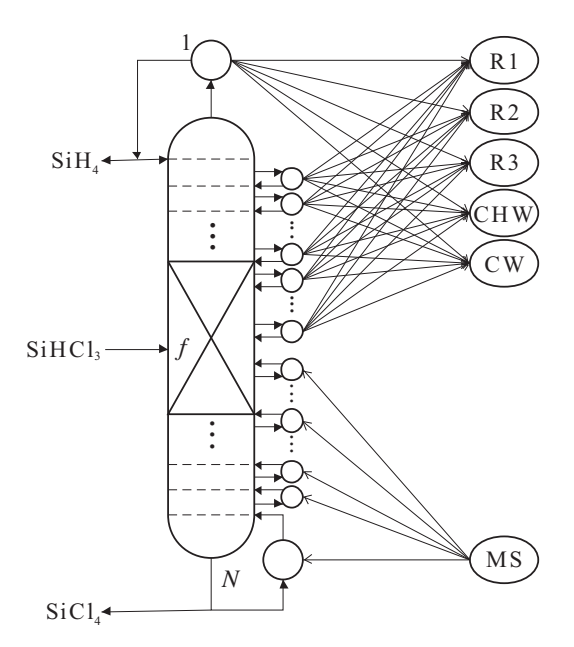


Fig. 3. Candidate cooling utilities for a reactive distillation column with two heat-integrated stages.



**Fig. 4.** Superstructure representation between a reactive distillation column and the candidate utilities.

The installation of inter-condensers or inter-reboilers does not remarkably change the equipment cost because the condenser and reboiler areas reduce as the ones in inter-condensers or interreboilers increase. However, since the use of refrigerants as cooling utilities results in very expensive operation cost, the cost of the reactive distillation column (RD) will be largely comprised by the operating cost. This subsection explains in detail the mathematical model to minimize the operation cost (*OC*) due to the installation of inter-condensers or inter-reboilers.

Eq. (9) shows the objective function implemented to minimize the operating cost

$$\min OC = OH \begin{bmatrix} \sum_{i \in REC} C_j^{\text{cool}} Q_{i,j}^{\text{ex}} + \sum_{i \in HU} C_i^{\text{heat}} Q_{i,j}^{\text{ex}} \\ j \in CU \qquad \qquad j \in STR \end{bmatrix}$$
(9)

where *REC* is the set of stages in the rectifying section subject to the installation of a condenser and inter-condensers, *STR* is the set of stages in the stripping section subject to the installation of a reboiler and inter-reboilers, *CU* is the set of cooling utilities, and *HU* is the set of heating utilities.  $C^{\rm cool}$  is the cost of cooling utilities while  $C^{\rm heat}$  is the cost of heating utilities.  $Q^{\rm ex}_{i,j}$  is the amount of heat exchanged between heat sources HSO (i.e.,  $HSO = REC \cup HU$ ) and heat sinks HSI (i.e.,  $HSI = STR \cup CU$ ). Finally, OH are the annual operation hours.

Changes in the condenser and reboiler duties due to heat integration at stages in a column can be predicted in advance from steady state simulations of a column without any heat integration as long as there are expressions which relate the heat removed or added at an stage and the effective condenser and reboiler duty reduction. One approximation is the use of compensation terms (Alcántara-Avila et al., 2013). They are explained in Eqs. (10) and (11)

$$Q^{cn} = Q_0^{cn} - \sum_{i \in REC} (Q_i^{sx} + \Delta Q_i^{sx}) - \sum_{j \in STR} \Delta Q_j^{sx}$$

$$\tag{10}$$

$$Q^{rb} = Q_0^{rb} - \sum_{i \in STR} (Q_j^{sx} - \Delta Q_j^{sx}) + \sum_{i \in REC} \Delta Q_i^{sx}$$

$$\tag{11}$$

where  $Q_0^{\rm cn}$  and  $Q_0^{\rm rb}$  are the condenser and reboiler duty before any heat integration and  $Q^{\rm cn}$  and  $Q^{\rm rb}$  are those values resulted from heat integration at stages.  $Q^{\rm sx}$  is the heat removed or supplied at stage i in the rectifying section or stage j in the stripping section by side exchangers while  $\Delta Q^{\rm sx}$  is the respective compensation term at a given stage subject to heat integration.  $\Delta Q^{\rm sx}$  are indicators of the inefficiency in the condenser and reboiler duty reduction resulted from heat integration. Therefore, large values must be avoided.

In this work, since the heat removal from the column takes negative values while the heat addition takes positive values, the signs in Eqs. (10) and (11) are different. In addition, since the compensation terms indicate the inefficiency in heat integration, they take only positive values. From the previous statement, it is worthy to notice that heat removal in the rectifying section results in an increase in the reboiler duty, and heat addition in the stripping section results in an increase in the condenser duty.

The compensation terms in the rectifying section due to heat removal is calculated by

$$\Delta Q_i^{\rm sx} \approx \Delta \hat{Q}_i^{\rm sx} = \max_{k \in PW} \left\{ a_{k,i} \delta_i + b_{k,i} Q_i^{\rm sx} \right\} \quad i \in \textit{REC}$$
 (12)

while the compensation terms in the stripping section due to heat addition is calculated by

$$\Delta Q_j^{\text{sx}} \approx \Delta \hat{Q}_j^{\text{sx}} = \max_{k \in PW} \left\{ a_{k,j} \delta_j + b_{k,j} Q_j^{\text{sx}} \right\} \quad j \in STR$$
 (13)

where  $\Delta \hat{Q}^{sx}$  is a piecewise linear function that approximates  $\Delta Q^{sx}$ . PW is the set of segments in the piecewise linear function.  $\delta$  is a dummy variable, which is zero when  $Q^{sx}$  is zero, and a and b are parameters in the linear functions. A thoroughly discussion of these equations can be found in the work of Alcántara-Avila et al. (2013).

The heat integration network between stages and heat sources is represented in the following equations. The heat removal from cooling utilities in the rectifying section is

$$\sum_{j \in CU} Q_{i,j}^{\text{ex}} = -Q_i^{\text{sx}} \quad i \in REC$$
(14)

while the heat addition from heating utilities in the stripping section is

$$\sum_{i \in HU} Q_{i,j}^{\text{ex}} = Q_j^{\text{sx}} \quad j \in STR$$
 (15)

In this work, the condenser and reboiler are considered stages in the column, thus the energy balance in Eqs. (10) and (11) is rewritten as follows

$$Q_1^{\text{sx}} = Q_0^{\text{cn}} - \sum_{i \in REC'} (Q_i^{\text{sx}} + \Delta Q_i^{\text{sx}}) - \sum_{i \in STR'} \Delta Q_j^{\text{sx}}$$

$$\tag{16}$$

$$Q_N^{\text{sx}} = Q_0^{\text{rb}} - \sum_{j \in STR'} (Q_j^{\text{sx}} - \Delta Q_j^{\text{sx}}) + \sum_{i \in REC'} \Delta Q_i^{\text{sx}}$$

$$\tag{17}$$

where *REC'* is the set of stages in the rectifying section excluding the condenser and *STR'* is the set of stages in the stripping section excluding the reboiler. Since the stages are counted from top to bottom in this research, the subscript 1 means the condenser location (top) and *N* is the reboiler location (bottom).

The log mean temperature difference ( $\Delta T_{\rm LM}$ ) is used to determine the temperature driving force for heat transfer in exchangers, and it is used as feasibility criterion for heat integration. Eq. (18) represents the  $\Delta T_{\rm LM}$  between heat sources and sinks while Eq. (19)

shows the feasibility criterion based on the "Big-M" formulation, which is a valid representation for linear constraints.

 $\Delta T_{\text{LM}i,j} = \begin{cases} \frac{(T_i^{\text{in}} - t_j^{\text{out}}) - (T_i^{\text{out}} - t_j^{\text{in}})}{T_i^{\text{out}} - t_j^{\text{out}}} & \text{if and} \\ 0 & \text{otherwise} \end{cases} \quad i \in \textit{HSO}, j \in \textit{HSI}(18)$ 

$$Q_{i,j}^{\text{ex}} - M\Delta T_{LMi,j} \le 0 \quad i \in HSO, j \in HSI$$
 (19)

where  $T^{in}$  and  $T^{out}$  are inlet and outlet temperature of the heat source i while  $t^{in}$  and  $t^{out}$  are inlet and outlet temperature of the heat sink j,  $\Delta T_{\min}$  is the minimum temperature difference allowed, and *M* is a big positive value.

Eq. (19) eliminates all infeasible heat exchanges because  $Q_{ij}^{ex}$ is zero when  $\Delta T_{LMi,i}$  is zero. The previous Eqs. (12)–(19) in this subsection can derive the best heat integration network between stages and utilities, however, since there is not a constraint to the number of heat exchanger, the number of heat integration would be the maximum possible. Eq. (20) is an additional constraint to enforce a determined number of heat exchangers in the rectifying and stripping sections

$$\sum_{i \in HSO} Y_{i,j}^{\text{ex}} \le N^{\text{ex}}$$

$$j \in HSI$$
(20)

where  $Y_{i,i}^{ex}$  is a binary variable which become one if a heat exchanger is installed between a heat source i and sink j, and zero otherwise, and Nex is a parameter which limits the maximum number of heat exchangers to be installed.

Additionally, Eq. (21) is necessary to allocate heat exchangers in feasible heat exchange networks

$$Q_{i,j}^{\text{ex}} - Y_{i,j}^{\text{ex}} Q_{\text{max } i,j}^{\text{ex}} \ge 0 \quad i \in HSO, j \in HSI$$
 (21)

where  $Q_{\max i,i}^{\text{ex}}$  is the upper bound for heat integration.

The solution of Eq. (9) subject to the constraints in Eqs. (12)–(21)presented in this subsection are used to find the heat integration network, which minimizes the operating cost for a designed reactive distillation column and a given number of heat exchangers. The presented equations are linear, therefore the solution of Mixed Integer Linear Programming (MILP) problems is valid to derive heat integration networks.

#### 3.2. Optimization procedure

In this subsection an iterative procedure, which combines the simulation software Aspen Plus V.8 and the optimization software IBM ILOG CPLEX Optimization Studio 12.5, is proposed and explained in detail.

Distillation is inherently characterized by a set of nonlinear and nonconvex equations. In the simulation software, these nonlinearities and nonconvexities are treated while in the optimization software, the combinatorial problem between heat exchangers and utilities which minimizes the operating cost is treated. The main reason to link these software is because, as mentioned in Section 3, the installation of inter-condensers or inter-reboilers in reactive distillation result in changes in the stage temperature, which affect the vapor-liquid equilibrium and reaction rate at the heat-integrated stage. Therefore, accurate calculations of the temperature profile, phase equilibrium and reaction rate are crucial.

Calculations of the temperature profile due to the installation of inter-condensers or inter-reboilers can result in very complex nonlinear mathematical expressions which imply the solution of complicated optimization problems which combine integer and

continuous variables. To avoid this situation, the temperature profile, phase equilibrium and reaction rate are successively updated

through an iterative procedure. Fig. 5 shows a flowchart for the proposed iterative procedure to find the best reactive distillation column with inter-condensers and/or inter-reboilers.

In this work, Microsoft Excel was used as interface and data handling software which is represented by the solid gray lines in Fig. 5. In the figure, the termination criterion is based on the Euclidean distance between changes in the heat removed and supplied by side heat exchangers at the sth iteration and that at the s + 1th iteration as shown in Eq. (22)

$$\sqrt{\sum_{i \in REC} (Q_{i,s}^{sx} - Q_{i,s+1}^{sx})^2 + \sum_{j \in STR} (Q_{j,s}^{sx} - Q_{j,s+1}^{sx})^2} \le \varphi$$
 (22)

where  $\varphi$  is a small number (e.g., 0.0001).

The initialization strategy for  $T_{i,s}^{\text{in}}$ ,  $T_{i,s}^{\text{out}}$ ,  $t_{j,s}^{\text{out}}$ ,  $Q_{j,s}^{\text{sx}}$ ,  $Q_{j,s}^{\text{sx}}$  will be discussed in detail in the results section. The results of each  $Q_{i,s}^{\text{sx}}$ ,  $Q_{j,s}^{\text{sx}}$  from the optimization software are input to the simulation software and, after execution, the new values for  $T_{is}^{in}$ ,  $T_{is}^{out}$ ,  $t_{is}^{in}$ ,  $t_{is}^{out}$ are input to the interface, then the updated values of the temperature are used to calculate the values of each element  $\Delta T_{\text{LM}i,j}$ , which are input to the optimization software, and the iteration loop is repeated until the termination criterion is satisfied.

The following equations are rather simple, but reasonable mathematical expressions to successively consider the changes in the

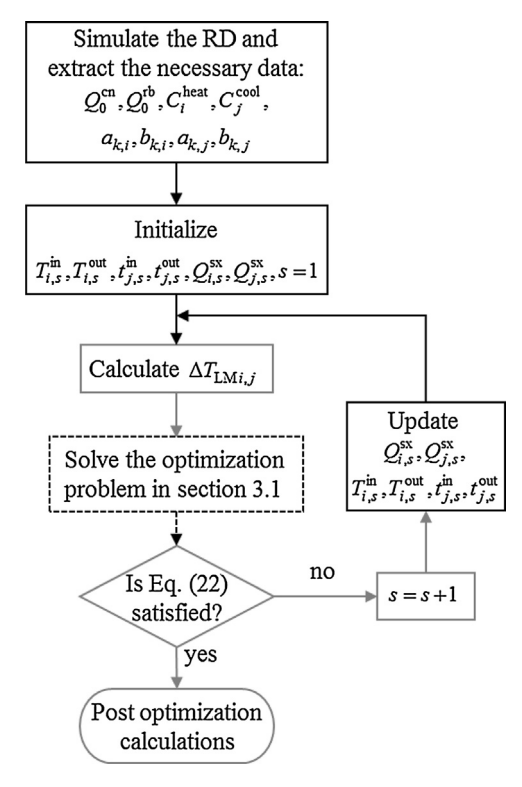


Fig. 5. Flowchart of the iterative optimization procedure: Simulation software (solid black lines), optimization software (dashed lines), interface (solid gray lines).

temperature profile along the rectifying and stripping sections. Eqs. (23) and (24) represent the temperature reduction in the rectifying section due to the installation of inter-condensers by taking the minimum temperature value at each stage through all the iterations

$$T_i^{\text{in}} = \min \left\{ T_{i,s}^{\text{in}} \right\} \quad i \in REC \tag{23}$$

$$T_i^{\text{out}} = \min\left\{T_{i,s}^{\text{out}}\right\} \quad i \in REC$$
 (24)

while Eqs. (25) and (26) represent the temperature increase in the stripping section due to the installation of inter-reboilers by taking the maximum temperature value at each stage through all the iterations

$$t_i^{\text{in}} = \max\left\{t_{i,s}^{\text{in}}\right\} \quad j \in STR \tag{25}$$

$$t_{j}^{\text{out}} = \max\left\{t_{j,s}^{\text{out}}\right\} \quad j \in STR$$
 (26)

#### 3.3. Post optimization calculations

Post optimization calculations are done to determine the equipment cost for the necessary heat exchangers derived from the optimization procedure in the previous subsection. The cost calculations were based on the Guthrie method (Turton et al., 2012). Egs. (27) and (28) are used to calculate the condenser, inter-condensers, reboiler, and inter-reboilers

$$A_{i,j}^{\rm cn} = \frac{Q_{i,j}^{\rm ex}}{U^{\rm cn}(\Delta T_{LMi,j} + \varepsilon)} \quad i \in REC, j \in CU$$
 (27)

$$A_{i,j}^{\text{rb}} = \frac{Q_{i,j}^{\text{ex}}}{U^{\text{rb}}(\Delta T_{LMi,j} + \varepsilon)} \quad i \in HU, j \in STR$$
 (28)

where A<sup>cn</sup> and A<sup>rb</sup> are the heat transfer area for condensers and reboilers,  $U^{cn}$  and  $U^{rb}$  are the overall heat transfer coefficients for condensers and reboilers, and  $\varepsilon$  is a small value (i.e., 0.0001) to avoid zero division if the heat exchange is infeasible.

#### 4. Results

In this section a discussion of the results obtained in this work

#### 4.1. Design of conventional reactive distillation columns

The typical reactive distillation column is a distillation column with some zones packed with the solid catalyst, which functions as mass transfer internals as well, and the coupled reaction and separation by distillation takes place at the same sites. In this paper, a typical reactive distillation column as shown in Fig. 1a was investigated first which composed of three sections: the rectifying, catalytic reaction and stripping sections, located at the upper, middle, and lower part, respectively, with the solid catalyst packed in the middle of the column. Trichlorosilane is fed into the column at the bottom of reaction section or the top of the stripping section. Then disproportionation takes place in the reaction section and vaporous product mixture containing light components ascend to the rectifying section while the heavy components descend to the stripping section. The intermediate products rise into the rectifying section but must return to the reaction section with the help of the top reflux flow, and the feed may flow down to the stripping section but back upward to the reaction section with the aid of the boilup stream from the bottom reboiler. This operational mode thus effectively make the overall reaction approach complete, and the most desired product silane is able to be withdrawn from the top of the column. To generate the optimal design, the number of stages in the column, the number of reactive stages, the position of the reactive

Additional optimization and post optimization parameters.

M(-)	50	
OH (h/year)	8500	
PB (year)	10	
U <sup>cn</sup> (kW/m <sup>2</sup> K)	0.568	
$U^{\rm rb}$ (kW/m <sup>2</sup> K)	0.454	
$A_{\min}^{\rm cn}$ (m <sup>2</sup> )	3	
$A_{\min}^{\text{cn}}$ (m <sup>2</sup> ) $A_{\min}^{\text{rb}}$ (m <sup>2</sup> )	10	
$\Delta T_{\min}$ (K)	8	
$Q_{\max i,j}^{ex}$ (kW)	450 <sup>*</sup>	
$N^{ex}(-)$	{2,3,4}	

<sup>\*</sup> The values of  $Q_{\max 1,j}^{\text{ex}}$   $j \in CU$  and  $Q_{\max i,N}^{\text{ex}}$   $i \in HU$  were set to 1000 to warranty feasibility in conventional reactive distillation.

stage, the position of the feed stage, the reflux ratio and the operating pressure were manipulated. The objective function for this procedure was to generate the design with minimum total annual cost. The optimal reactive distillation scheme was obtained with a 64 stages. The reaction section was from stage 16 to stage 45, with a liquid residence time of 2.5 s on each stage which is defined as hold-up/liquid-flow-rate. The column is operated at a top pressure of 506.625 kPa with a pressure drop through each stage of 0.5 kPa. The purity of silane in distillate in mole fraction is 0.99. Trichlorosilane at 10 kmol/h was fed into the column on stage 26 at 50 °C and 557.28 kPa.

#### 4.2. Optimization of reactive distillation columns with heat-integrated stages

The procedure proposed in Section 3.2 was adopted to generate the solutions presented in this subsection. Table 4 shows the additional parameters to perform the optimization and post optimization calculations.

The following equations are added to the optimization problem in Section 3.1 to enforce the existence of the top condenser and bottom reboiler. Eqs. (29) and (30) are set as lower limits for heat removal at the condenser or heat addition at the reboiler, respectively.

$$Q^{cn} = Q_1^{sx} \le -A_{min}^{cn} U^{cn} \Delta T_{LMi,j} \quad i = 1, j = R1$$
 (29)

$$Q^{\rm rb} = Q_N^{\rm sx} \ge A_{\rm min}^{\rm rb} U^{\rm rb} \Delta T_{LMi,j} \quad i = MS, j = N$$
 (30)

where  $A_{\min}^{cn}$  is the minimum allowed area for the top condenser and  $A_{\min}^{rb}$  is the minimum allowed area for the bottom reboiler.

Eqs. (31) and (32) are used to calculate the equipment cost after the installation of inter-condensers or inter-reboilers.

$$EC = C^{\text{col}} + C^{\text{tray}} + \sum_{i \in HSO} C_{i,j}^{\text{ex}}$$

$$j \in HSI$$
(31)

$$TAC = EC/PB + OC (32)$$

where EC is the Equipment cost,  $C^{\rm col}$  is the cost of the column (vertical vessel),  $C^{\rm tray}$  is the tray cost, and  $C^{\rm ex}_{i,j}$  is the cost of heat exchangers including the top condenser and bottom reboiler. PB is the payback time, and TAC is the total annual cost of the resulting reactive distillation column. Here also, the cost calculations were based on the Guthrie method (Turton et al., 2012).

Because there are complex nonlinear relations between the locations and amount of heat transferred in the exchangers, four initialization methods were investigated to solve the optimization problem:

- 1. Initialize all  $Q_i^{sx}=0$ ,  $Q_j^{sx}=0$   $i\in REC', j\in STR'$ 2. Initialize randomly all  $Q_i^{sx}$ ,  $Q_j^{sx}$   $i\in REC', j\in STR'$

**Table 5**Optimization results.

Solution	N <sup>ex</sup> = 2 (Conventional RD)	N <sup>ex</sup> = 3 (1 Inter-condenser)	N <sup>ex</sup> = 4 (2 Inter-condensers)	Relaxed solution
$\sum C_{j}^{\text{cool}} Q_{i,j}^{ex} \left( \text{$/$year} \right)$	588,613	134,173	60,012	59,376
$i \in REC$ $i \in CU$				
$\sum C_i^{\text{heat}} Q_{i,j}^{\text{ex}} (\$/\text{year})$	213,262	213,262	265,971	265,971
$i \in HU$ $j \in STR$				
OC (\$/y)	801,875	347,435	325,983	325,347
$\sum C_{1,j}^{ex}$ Condenser (\$)	60,993	3783	3783	3783
$\sum_{C^{eX}} C^{eX} Pahailan(C)$	C4 247	C4 240	71.074	71.074
$\sum_{i \in HU} C_{i,N}^{ex} \text{ Reboiler (\$)}$	64,247	64,248	71,974	71,974
$\sum C_{i,j}^{ex}$ Exchangers (\$)	0	54,217	87,878	79,099
i ∈ HSO′				
$j \in HSI'$				
C <sup>col</sup> (\$)	171,204	171,204	171,204	171,204
$C^{\text{tray}}$ (\$)	94,536	94,536	94,536	94,536
EC (\$)	390,980	387,988	429,375	420,596
TAC (\$/year)	840,973	386,234	368,921	367,407

- 3. Initialize randomly all  $Q_i^{sx}$ ,  $Q_i^{sx}$  only in the reaction section
- Initialize the problem by solving the relaxed MILP (RMILP) and using the temperature profile of the conventional reactive distillation column.

From the above initialization methods, the RMILP was the one which obtained the final configurations with less iterations.

The iterative procedure applied to the RMILP was done by replacing the binary variables with continuous variables between 0 and 1. The solution of RMILP represents the lower bound of the optimization problem in Section 3.1. In the relaxed solution, only the bottom reboiler was selected in the stripping section, which implies that the installation of inter-reboilers does not reduce the

operating cost, this result make sense because  $\sum_{j \in \mathit{STR'}} \Delta \mathit{Q}_j^{\mathit{sx}}$  will be

higher than zero if an inter-reboiler is installed, thus the cooling cost will increase.

Table 5 shows the optimization results for the conventional RD, the RD with one and two inter-condensers, and the relaxed solution (RMILP). The installation of 1 inter-condenser reduces 56% the *OC* and 54% the *TAC* while the installation of 2 inter-condensers reduces 59% the *OC* and 56% the *TAC*.

The relative differences between the relaxed solution and the case where 2 inter-condensers are installed in terms of *OC* and *TAC* are within 0.2% and 0.4%, respectively. Therefore, these results imply that the increase in the number of inter-condensers will not

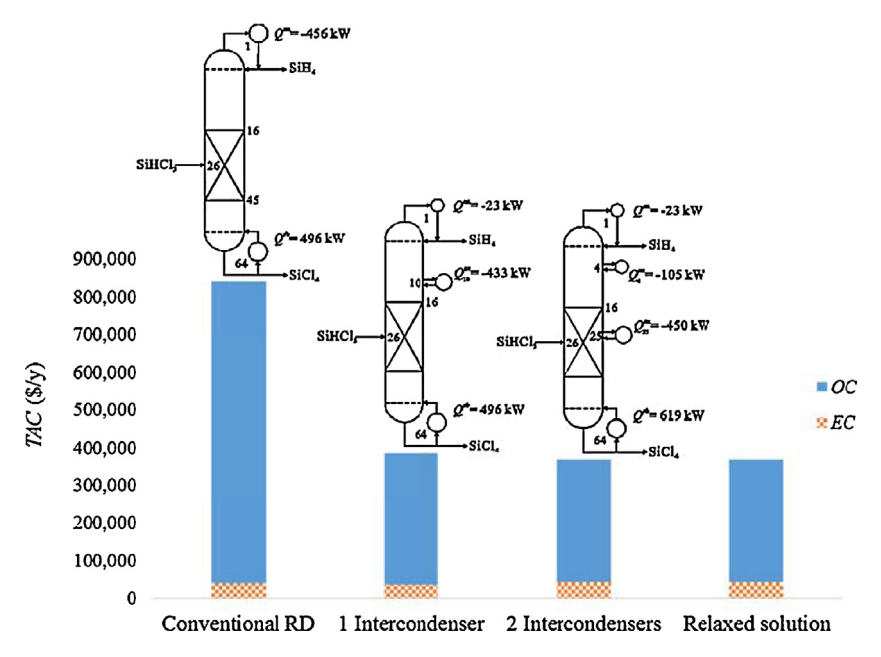


Fig. 6. Optimal solutions of reactive distillation columns with inter-condensers.

remarkably improve the optimal solution. Therefore the maximum number of installed inter-condensers is 2.

The installation of one inter-condenser also reduces the equipment cost when compared with the conventional case, this situation emphasizes another advantage of heat-integrated stages because heat exchangers of smaller size can be used since the temperature difference between stages and utilities is higher than that between the condenser and utilities. The installation of two condensers, however, resulted in 10% increase in the equipment cost because of the large size in the second condenser ( $45.2\,\mathrm{m}^2$ ) and an increase in the reboiler size ( $32.3\,\mathrm{m}^2$ ).

Fig. 6 shows the optimal reactive distillation columns with intercondensers. When one inter-condenser is allowed, the best location is stage 10 and when two inter-condensers are allowed, the best locations are stages 4 and 25. The heat removed at stage 25 is at the upper bound of  $Q_{\max i,j}^{\rm ex}$  (450 kW at stages in the rectifying section), this is because water is used as cooling source, which is the cheapest cooling utility.

#### 5. Conclusions

It has been proved that it is feasible to obtain a high purity of silane over 99% and a complete conversion of trichlorosilane to silane by a typical reactive distillation column. The heat removal and addition at stages result in changes of the temperature profile inside the reactive column. In this work, an optimization procedure was proposed to deal with these changes by iteratively updating the temperature profile and heat integration network through rigorous simulations. In the optimization, the combinatorial problem between stages and utilities was solved while in the simulation; the synthesis problem for the obtained optimal heat integration network was solved. The key feature to derive optimal heat integration networks strongly depends on the accurate estimation of changes in the condenser and reboiler energy requirements due to heat integration, for these purposes, the concept of compensation terms was effectively adopted.

Among the four initialization methods that were studied, the initialization by solving the relaxed optimization problem was the fastest one to reach the final solution. The relaxed solution of the optimization problem showed that the installation of interreboilers does not yield to economic savings in the operation or equipment cost. In addition, the relative gap was 0.2% between the relaxed solution and the case where two inter-condensers were installed; therefore, the latter case was set as the best solution.

#### Acknowledgements

The authors acknowledge for the financial support to this work by Universidad de Guanajuato, CONACYT (Mexico) Grant No. 385/2014 and for the academic support by Tokushima University.

#### References

Alcántara-Avila JR, Kano M, Hasebe S. New synthesis procedure to find the optimal distillation sequence with internal and external heat integrations. Ind Eng Chem Res 2013:52:4851.

Bakay CJ. Process for making silane. U.S. Patent 3,968,199; 1976.

Block H, Leimkuehler H, Mueller D, Schaefer J, Ronge G. Method and system for producing silane. U.S. Patent 6,905,576; 2005.

Braga AFB, Moreira SP, Zampieri PR, Bacchin JMG, Mei PR. New processes for the production of solar-grade polycrystalline silicon: a review. Sol Energy Mater Sol Cells 2008:92:418.

Breneman WC. High purity silane and silicon production. U.S. Patent 4,676,967; 1987.

Breneman WC. Process for production of silane and hydrohalosilanes. U.S. Patent 0156675 A1; 2013.

Carrera-Rodríguez M, Segovia-Hernández JG, Bonilla-Petriciolet A. Short-cut method for the design of reactive distillation columns. Ind Eng Chem Res 2011;50:10730.

Flagella RN. Fluidized bed for production of polycrystalline silicon. U.S. Patent 5,139,762; 1992.

Frings AJ. Continuous catalytic process for the production of dichlorosilane. In: Proceedings of silicon for the chemical industry V; 2000.

Fthenakis V, Mason J, Zweibel K. The technical, geographical and economic feasibility for solar energy to supply the energy needs of the United States. Energy Policy 2009:37:387.

Huang X, Ding WJ, Yan JM, Xiao WD. Reactive distillation column for disproportionation of trichlorosilane to silane: reducing refrigeration load with intermediate condensers. Ind Eng Chem Res 2013;52:6211.

Inoue K. A Simple process for the production of monosilane. JP01317144; 1988. Iya SK. Reactor for fluidized bed silane decomposition. U.S. Patent 4,818,495;

1989. Li KY. Redistribution reaction of trichlorosilane in a fixed-bed reactor. Ind Eng Chem

Matthes R, Schrok R, Vahlesieck HJ. Method for the preparation of dichlorosilane. EP 0474265; 1988.

Müller D, Ronge G, Schäfer JP, Leimküler HJ. Development and economic evaluation of a reactive distillation process for silane production. In: Proceedings of the International Conference on Distillation and Absorption; 2002, 4-1.

Müller A, Ghosh M, Sonnenschein R, Woditsch P. Silicon for photovoltaic applications. Mater Sci Eng B Adv Funct Solid State Mater 2006;134:257.

Muller D, Ronge G, Schaefer J, Leimkkuehler H, Strauss U, Block H. Method and facility for producing silane. U.S. Patent 6,942,844; 2005.

Parida B, Iniyan S, Goic R. A review of solar photovoltaic technologies. Renew Sustain Energy Rev 2011;15:1625.

Sonnenschein R, Adler P, Popken T, Kahsnitz J. Apparatus and process for preparing silanes. U.S. Patent 8,038,961; 2011.

Turton R, Bailie RC, Whiting WB, Shaeiwitz JA, Bhattacharyya D. Analysis synthesis and design of chemical processes. 4th ed. USA: Prentice Hall; 2012.

Sundmacher K, Kienle A. Reactive distillation: status and future direction. 1st ed. Germany: Wiley; 2003.

Yamada M, Ishii S, Nakajima T. Method of continuous production of silanes. IP121110: 1984.